Supplement of Biogeosciences, 21, 3691–3716, 2024
https://doi.org/10.5194/bg-21-3691-2024-supplement


Biogeosciences
Open Access

*Supplement of*

# Modeling integrated soil fertility management for maize production in Kenya using a Bayesian calibration of the DayCent model

**Moritz Laub et al.**

*Correspondence to:* Moritz Laub (moritz.laub@usys.ethz.ch)

## S1 Pedotranfer functions to derive the hydraulic parameters

The equations used to calculate the soil hydraulic properties were based on the pedotransfer functions of Hodnett and Tomasella (2002):

$$\theta_r = 0.22733 - 0.00164 \times Sa + 0.00235 \times CEC - 0.00831 \times pH + 1.8 \times 10^{-5} \times Cl^2 + 2.6 \times 10^{-5} \times Sa \times Cl \tag{S1}$$

$$\theta_s = 0.81799 + 9.9 \times 10^{-4} \times Cl - 0.3142 \times BD + 1.8 \times 10^{-4} \times CEC + 0.00451 \times pH - 5 \times 10^{-6} \times Sa \times Cl \tag{S2}$$

$$ln(\alpha) = -0.02294 - 0.03526 \times Si + 0.024 \times SOC - 7.6 \times 10^{-3} \times CEC - 0.11331 \times pH \tag{S3}$$

$$ln(n) = 0.62986 - 0.00833 \times Cl - 0.00529 \times SOC + 0.00593 \times pH + 7 \times 10^{-5} \times Cl^2 - 1.4 \times 10^{-4} \times Sa \times Si \tag{S4}$$

Here, $\theta_r$, $\theta_s$, $\alpha$, and $n$ are the soil water retention parameters of van Genuchten (1982), *Sa*, *Si* and *Cl* are Sand, Silt, and Clay content (in %), *BD* is the bulk density (t $m^{-3}$) CEC is the cation exchange capacity (cmol $kg^{-1}$), *pH* is the soil pH measured in $H_2O$, and *SOC* is the SOC content (g $kg^{-1}$).

The wilting point (WP) and field capacity (FC) values were then calculated as

$$WP = \theta_r + \frac{(\theta_s - \theta_r)}{(1 + (\alpha \times |-15000|)^n)^{1-\frac{1}{n}}} \tag{S5}$$

$$FC = \theta_r + \frac{(\theta_s - \theta_r)}{(1 + (\alpha \times |-330|)^n)^{1-\frac{1}{n}}} \tag{S6}$$

$K_S$ was calculated using the Saxton and Rawls (2006) equation, with values of the water retention curve, $\alpha$ and *n* (van Genuchten, 1982), calculated with the equation from Hodnett and Tomasella (2002):

$$\lambda = \frac{\ln(FC) - \ln(WP)}{\ln(1500) - \ln(33)} \tag{S7}$$

$$K_S = \frac{1930 \times (\theta_s - FC)^{(3-\lambda)}}{10 \times 60 \times 60} \tag{S8}$$

Here, $\lambda$ is the slope of logarithmic tension-moisture curve and $K_S$ is the saturated water conductivity (cm $s^{-1}$).

## S2 Equations for the global sensitivity analysis

The means across all sites, which were used in the GSA were calculated as follows:

$$Mean = \frac{1}{n} \sum_{j=1}^{n} \frac{\sum_{i=1}^{N} Mod_{ij}}{N} \tag{S9}$$

Here $n$ is the number of sites (4), $N$ is the number of modelled values per site, and $Mod_{ij}$ are the individually modelled values. For aboveground biomass and grain yield, $N$ corresponded to the total number of modelled yields and biomass at all treatments and seasons. For SOC and soil N stock $N$ corresponded to the total number of treatments per site. The reason is that because changes in SOC and soil N stocks are expected to be stronger the longer a simulation lasts, only the stocks from the end of the simulation were used.

## S3 Supplementary tables

**Table S1.** Locations, soil properties and climatic conditions of the study sites. Soil properties are given for the 0 - 15 cm depth layer. Coordinates are given in the WGS 84 reference system. The table is adopted from Laub et al. (2022) under the creative common license 4: http://creativecommons.org/licenses/by/4.0/.

| Soil characteristics | Embu | Machanga | Sidada | Aludeka |
|---|---|---|---|---|
| Latitude | -0.517 | -0.793 | 0.143 | 0.574 |
| Longitude | 37.459 | 37.664 | 34.422 | 34.191 |
| Initial soil C (%) | 3.1 | 0.8 | 2.6 | 0.7 |
| Initial N (%) | 0.3 | 0.05 | 0.21 | 0.06 |
| Initail bulk density (g $cm^{-3}$) | 1.26 | 1.51 | 1.3 | 1.45 |
| pH ($H_2O$) | 5.43 | 5.27 | 5.4 | 5.49 |
| Sand (%) | 0 | 31.1 | 0.1 | 31 |
| Clay (%) | 59.8 | 13.2 | 55.7 | 13.4 |
| Soil type (FAO, 1998) | Humic Nitisol | Ferric Alisol | Humic Ferralsol | Acrisol |
| Altitude (m)* | 1380 | 1022 | 1420 | 1180 |
| Annual rainfall (mm)* | 1175 | 795 | 1730 | 1660 |
| Mean annual temperature (°C) | 20.1 | 23.7 | 22.6 | 24.4 |
| Months of long rainy season | 3 - 8 | 3 - 8 | 3 - 9 | 3 - 9 |
| Months of short rainy season | 10 - 01 | 10 - 01 | 10 - 01 | 10 - 01 |

*Means calculated based on measured data from 2005 to 2020

**Table S2.** Mean measured chemical characteristics (and 95% confidence intervals) of organic resources applied at all sites. Measurements were available from Embu and Machanga from 2002 to 2004, all sites from 2005 to 2007 and in 2018. Significant differences in residue properties were found between the different organic resources, but not between sites and years. Mean values in a row not sharing any lowercase letter are significantly different from each other ($p < 0.05$). Abbreviations: n.c. = not classified * according to Palm et al. (2001). The table is adopted from Laub et al. (2023) under the creative common license 4: http://creativecommons.org/licenses/by/4.0/.

| Measured property | *Tithonia* | *Calliandra* | Maize stover | Sawdust | Farmyard manure |
|---|---|---|---|---|---|
| C (g $kg^{-1}$) | $345^{b}$ (333-357) | $396^{c}$ (383-409) | $397^{c}$ (386-408) | $433^{d}$ (416-449) | $234^{a}$ (213-255) |
| N (g $kg^{-1}$) | $33.2^{d}$ (28.9-38.2) | $32.5^{d}$ (28.3-37.3) | $7.2^{b}$ (6.5-8) | $2.5^{a}$ (2.1-2.8) | $18.1^{c}$ (15-21.8) |
| C/N ratio | $12.4^{a}$ (10.8-14.1) | $13.6^{a}$ (11.9-15.5) | $58.7^{b}$ (52.8-65.2) | $199.1^{c}$ (174.1-227.7) | $12.3^{a}$ (9.9-15.4) |
| P (g $kg^{-1}$) | $2.3^{d}$ (1.8-2.9) | $1.1^{c}$ (0.8-1.5) | $0.4^{b}$ (0.3-0.6) | $0.1^{a}$ (0-0.2) | $3.1^{d}$ (2.3-3.9) |
| K (g $kg^{-1}$) | $37.2^{c}$ (21.2-65.2) | $8.7^{b}$ (5-15.3) | $9^{b}$ (6-13.5) | $2.8^{a}$ (1.6-4.9) | $19.4^{bc}$ (7.8-48.6) |
| Lignin (g $kg^{-1}$) | $90^{ab}$ (62-117) | $105^{b}$ (77-133) | $48^{a}$ (37-60) | $172^{c}$ (144-199) | $198^{c}$ (154-242) |
| Polyphenols (g $kg^{-1}$) | $19^{c}$ (14.9-24.3) | $108.7^{d}$ (85.3-138.6) | $11.3^{b}$ (9.5-13.6) | $4.9^{a}$ (3.8-6.2) | $7.8^{ab}$ (5.2-11.5) |
| Lignin/N ratio | $2.6^{a}$ (1.8-3.7) | $3.1^{ab}$ (2.2-4.3) | $6.2^{c}$ (4.8-8) | $58.3^{d}$ (41.1-82.8) | $6.9^{bc}$ (3.9-12.3) |
| Quality / turnover rate* | High / fast | High / slow | Low / fast | Low / slow | n.c. |
| Class* | 1 | 2 | 3 | 4 | n.c. |
| kg N in 4.0 t C $ha^{-1}$ $yr^{-1}$, -N [+N] | 323 [563] | 295 [535] | 68 [308] | 20 [260] | 324 [564] |
| kg N in 1.2 t C $ha^{-1}$ $yr^{-1}$, -N [+N] | 97 [337] | 88 [328] | 20 [260] | 6 [246] | 97 [337] |

**Table S3.** DayCent model parameters (and feasible ranges) of parameters which were not included in the Bayesian model calibration due to a Sobol total sensitivity index < 1%.

| Parameter | Description | Range width | Units | Initial value | Coefficient of variation | Model file |
|---|---|---|---|---|---|---|
| frtc(2) | C allocated to roots at time frtc(3) without stress | small | fraction of NPP | 0.20 | 0.15 | crop.100 |
| frtc(4) | Max. increase in C going to roots under stress | small | fraction of NPP | 0.10 | 0.15 | crop.100 |
| frtc(5) | Max. increase in C going to roots under stress (maturity) | small | fraction of NPP | 0.10 | 0.15 | crop.100 |
| biomax | AGB at which min.and max. C/E ratios of plant increases | small | g biomass $m^{-2}$ | 700.00 | 0.15 | crop.100 |
| pramx(1,2) | Max. aboveground C/N ratio with biomass > biomax | small | C/N ratio | 125.00 | 0.15 | crop.100 |
| prbmn(1,1) | For computing min. C/N ratio for belowground matter | small | C/N ratio | 45.00 | 0.15 | crop.100 |
| efrgrn(1) | Fraction of above ground N which goes to grain. | small | fraction | 0.75 | 0.15 | crop.100 |
| flig(1,1) | Intercept for annual rainfall effect on lignin content | small | fraction of lignin | 0.12 | 0.15 | crop.100 |
| ppdf(3) | Right curve shape for temperature effect on growth curve | very small | unitless | 1.00 | 0.08 | crop.100 |
| ppdf(4) | Right curve shape for temperature effect on growth curve | very small | unitless | 2.50 | 0.08 | crop.100 |
| favail(1) | Fraction of N available per day to plants | moderate | fraction of N | 0.15 | 0.23 | crop.100 |
| (aneref(1)-anaref(2)) | Rain/ET ratio below which, no effect of anaerobiosis | small | unitless | 1.00 | 0.15 | fix.100 |
| aneref(2) | Rain/ET ratio with max. anaerobiosis effect | moderate | unitless | 3.00 | 0.23 | fix.100 |
| damr(1,1)&(2,1) | Fraction of surface N and soil N absorbed by residue | large | fraction of N | 0.02 | 0.38 | fix.100 |
| damrmn(1) | Min. C/N ratio allowed in residue after direct absorption | moderate | C/N | 15.00 | 0.23 | fix.100 |
| dec1(2) | Max. structural litter turnover | small | g $g^{-1}$ $yr^{-1}$ | 4.90 | 0.15 | fix.100 |
| dec2(2) | Max. metabolic litter turnover | small | g $g^{-1}$ $yr^{-1}$ | 18.50 | 0.15 | fix.100 |
| dec3(2) | Max. active pool turnover | small | g $g^{-1}$ $yr^{-1}$ | 7.30 | 0.15 | fix.100 |
| (decX(2)/decX(1)) | Ratio soil to surface turnover (newly defined parameter) | small | unitless | 1.25 | 0.15 | fix.100 |
| fwloss(1) | Scaling factor; interception & evaporation by biomass | moderate | unitless | 1.00 | 0.23 | fix.100 |
| fwloss(2) | Scaling factor; bare soil precipitation evaporation | moderate | unitless | 1.00 | 0.23 | fix.100 |
| fwloss(3) | Scaling factor; transpiration water loss | moderate | unitless | 1.00 | 0.23 | fix.100 |
| pabres | Residue amount which results in max. direct N absorption | moderate | g C $m^{-2}$ | 100.00 | 0.23 | fix.100 |
| teff(2) | Y location of temperature inflection point (decomposition) | large | unitless | 11.75 | 0.38 | fix.100 |
| teff(3) | Step size of temperature effect on decomposition | moderate | unitless | 29.70 | 0.23 | fix.100 |
| teff(4) | Inflection point slope of temperature effect (decomposition) | very large | unitless | 0.25 | 0.45 | fix.100 |
| varat11&12(1,1) | Max. C/N ratio for material entering active pool | small | C/N | 20.00 | 0.15 | fix.100 |
| varat11&12(2,1) | Min. C/N ratio for material entering active pool | small | C/N | 3.00 | 0.15 | fix.100 |
| varat21&22(1,1) | Max. C/N ratio for material entering slow pool | small | C/N | 20.00 | 0.15 | fix.100 |
| varat3(1,1) | Max. C/N ratio for material entering passive pool | small | C/N | 13.00 | 0.15 | fix.100 |
| varat3(2,1) | Min. C/N ratio for material entering passive pool | small | C/N | 6.00 | 0.15 | fix.100 |
| drain | Fraction of excess water lost by drainage | moderate | fraction of $H_2O$ | 0.80 | 0.23 | site.100 |
| dmp_st | Damping factor for calculating soil temperature by layer | large | unitless | 0.01 | 0.38 | sitepar.in |
| N2Oadjust_(max-min) | Proportion of nitrified N that is lost as $N_2O$ (difference) | large | fraction of N | 0.003 | 0.38 | sitepar.in |
| Ncoeff | Min water/temperature limitation coefficient (nitrification) | large | unitless | 0.03 | 0.38 | sitepar.in |
| dmpflux | The damping factor for soil water flux | large | unitless | 0.00 | 0.38 | sitepar.in |
| astlig_TD | lignin fraction content of organic matter | small | g $g^{-1}$ biomass | 0.09 | 0.15 | omad.100 |
| astrec(1)_TD | C/N ratio of added organic matter | very small | C/N ratio | 12.40 | 0.08 | omad.100 |
| astlig_CC | lignin fraction content of organic matter | small | g $g^{-1}$ biomass | 0.10 | 0.15 | omad.100 |
| astrec(1)_CC | C/N ratio of added organic matter | very small | C/N ratio | 13.60 | 0.08 | omad.100 |
| astlig_MS | lignin fraction content of organic matter | small | g $g^{-1}$ biomass | 0.05 | 0.15 | omad.100 |
| astrec(1)_MS | C/N ratio of added organic matter | very small | C/N ratio | 58.70 | 0.08 | omad.100 |
| astlig_SD | lignin fraction content of organic matter | small | g $g^{-1}$ biomass | 0.17 | 0.15 | omad.100 |
| astrec(1)_SD | C/N ratio of added organic matter | very small | C/N ratio | 199.10 | 0.08 | omad.100 |
| astlig_FYM | lignin fraction content of organic matter | small | g $g^{-1}$ biomass | 0.20 | 0.15 | omad.100 |
| astrec(1)_FYM | C/N ratio of added organic matter | small | C/N ratio | 12.30 | 0.15 | omad.100 |

## S4 Supplementary figures

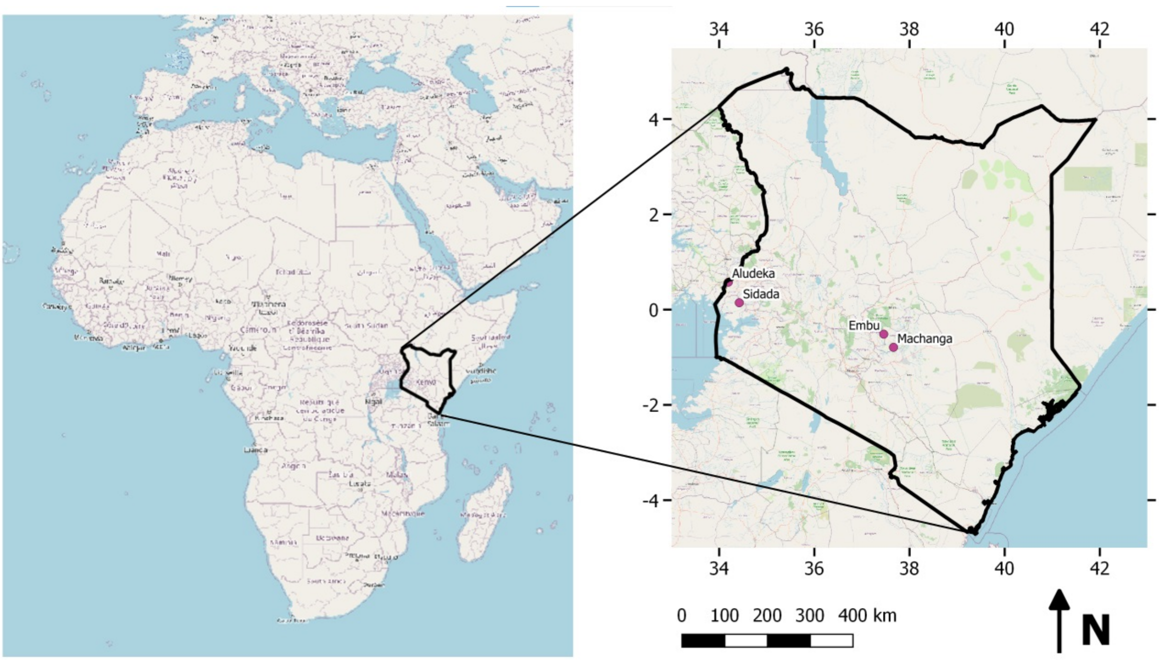


**Figure S1.** Map displaying the location of the four study sites. Background map data from ©OpenStreetMap contributors 2023. Distributed under the Open Data Commons Open Database License (ODbL) v1.0.

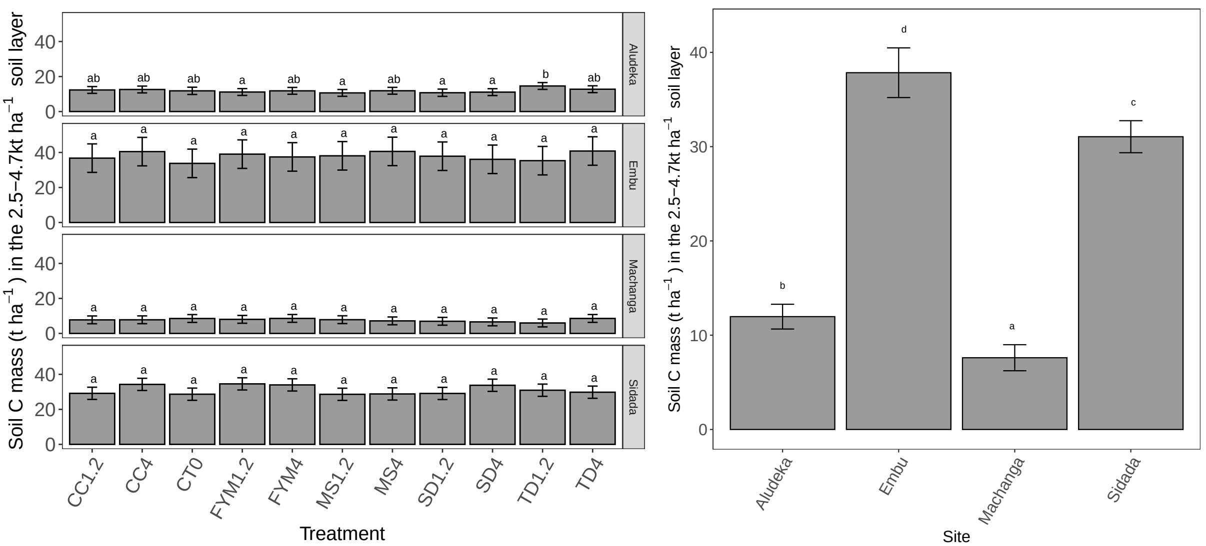


**Figure S2.** Subsoil SOC stocks for the 2.5-4.7 kt ha$^{-1}$ equivalent soil mass layer, corresponding to an approximate soil depth of 15-30 cm. Displayed are the least square means estimated by the linear mixed model described in (Laub et al., 2023) for planted plots by treatment (left) and site (right). Error bars display the 95% confidence intervals. Mean values at each site not sharing any lowercase letter are significantly different from each other (left figure). In the right figure, mean values per site not sharing any lowercase letter are significantly different from each other (all $p < 0.05$). Abbreviations: CC, *Calliandra*; CT, control; FYM, farmyard manure; MS, maize stover; SD, sawdust; TD, *Tithonia Diversifolia*. 0, 1.2 and 4 correspond to C additions of 0, 1.2 and 4 t C ha$^{-1}$ yr$^{-1}$.

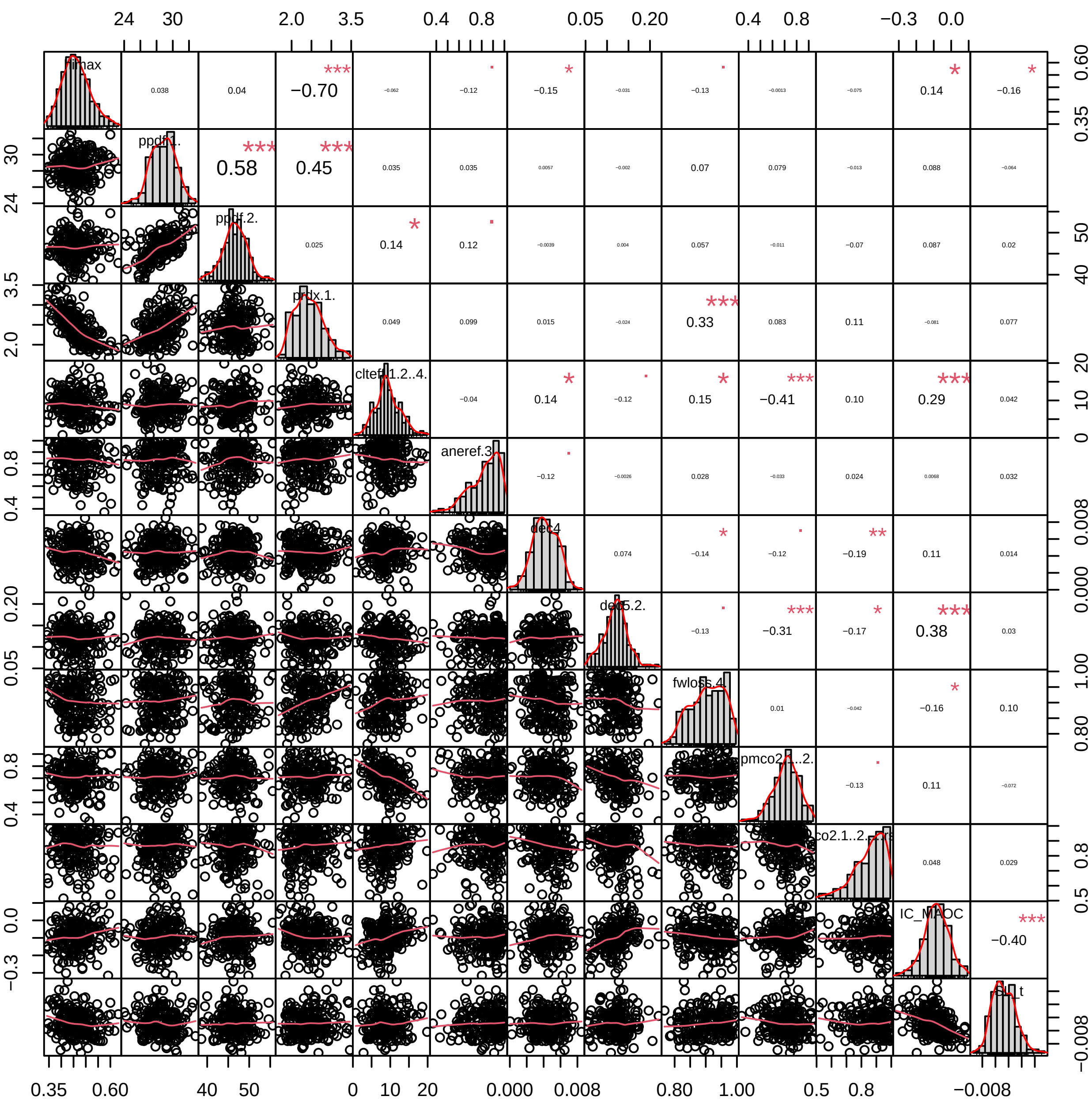

**Figure S3.** Correlation of parameters from the posterior parameter sets. The posterior distributions are based on all four sites combined.

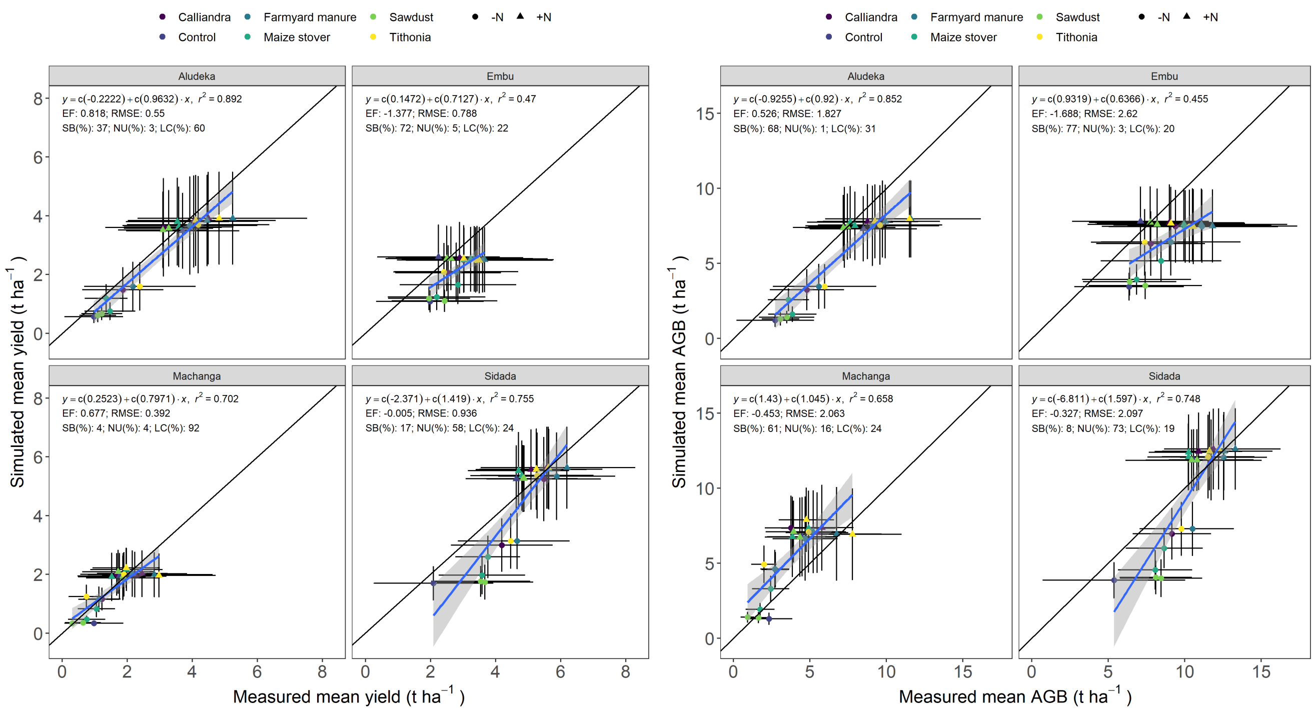


**Figure S4.** Mean simulated versus measured yield and aboveground biomass (AGB) from the leave-one-site-out cross-validation. Error bars represent the standard deviation of measured and simulated values over all years. Abbreviations: EF, Nash-Sutcliffe model efficiency; RMSE, root mean squared error; SB, squared bias; NU, non-unity slope; LC, lack of correlation. Across all sites model statistics: EF, 0.760; RSME, 0.699 t ha$^{-1}$; SB, 28%; NU, 8%; LC, 64% for yield; EF, 0.513; RSME, 2.17 t ha$^{-1}$; SB, 10%; NU, 9%; LC, 81% for AGB.

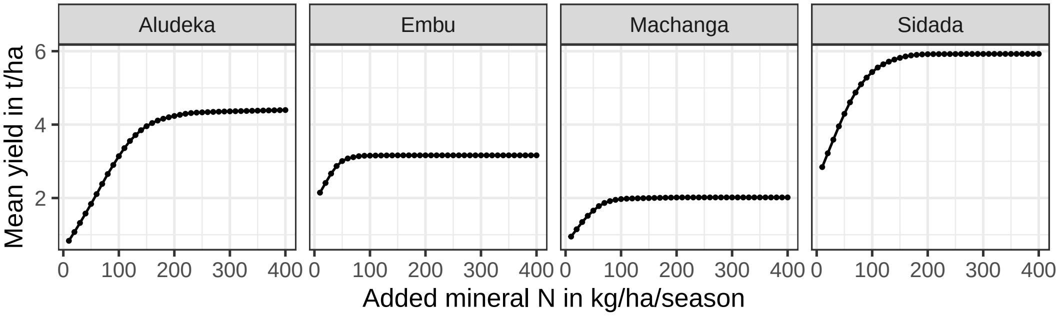


**Figure S5.** Yield response curve of DayCent to varying levels of mineral N application (control + N treatment, without organic resources) using the calibrated DayCent parameters. Displayed are the simulated mean yields across all simulated seasons (32 at Sidada and Aludeka, 38 seasons at Embu and Machanga). The amount of mineral N applied per season in the simulations was evenly split between the actual application dates of mineral N in each season at each site.

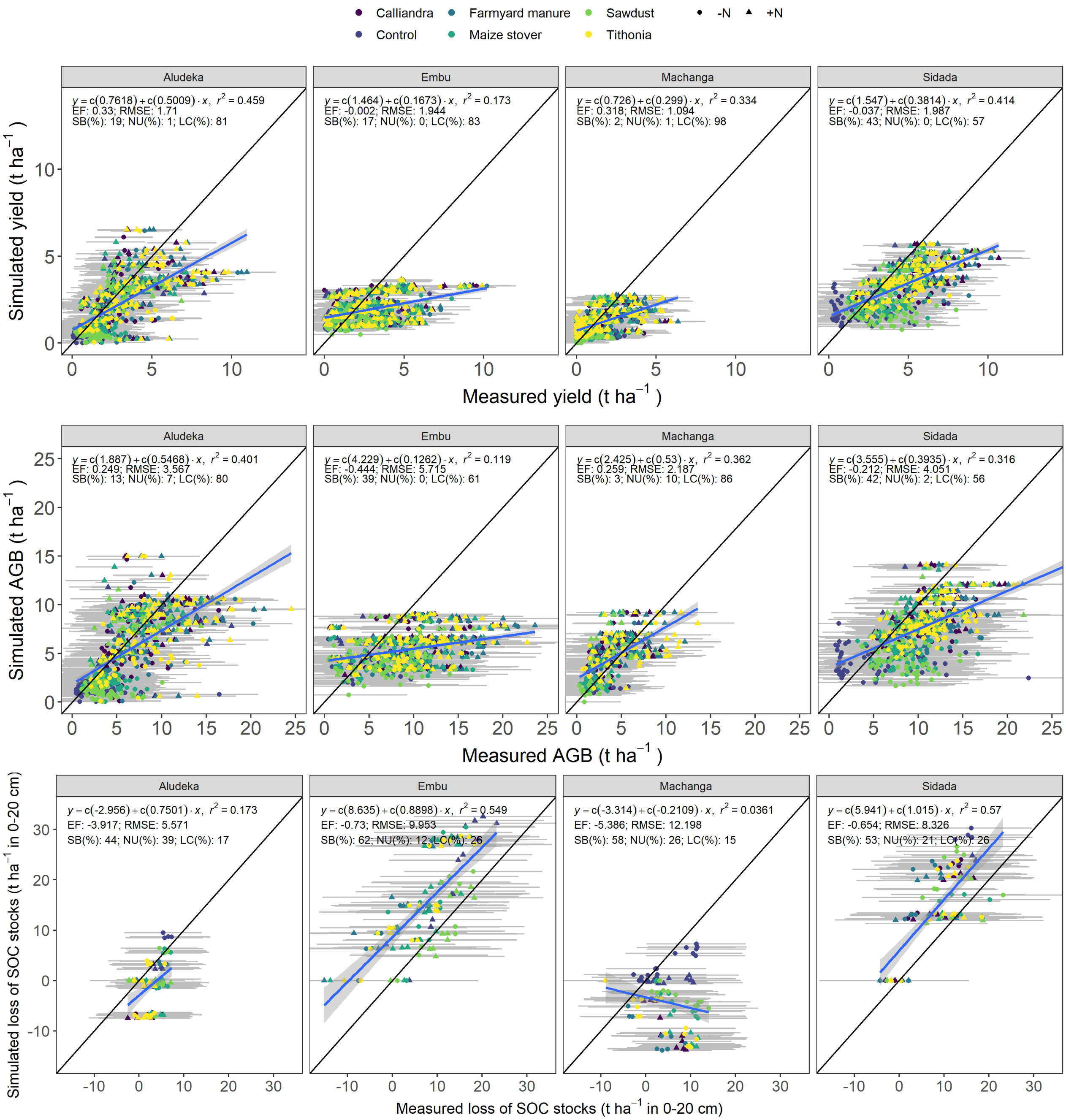


**Figure S6.** Simulated compared to measured maize grain yields, abovoground biomass and change in SOC stocks at the four study sites for the default DayCent parameter set before adjusting ps1co(1&2)&rsplig from 0.5 to 0.85. Grey bands show the 95% confidence intervals of measured (horizontal) values and the 95% credibility intervals of posterior distribution (vertical). Abbreviations: EF, Nash-Sutcliffe model efficiency; RMSE, root mean squared error; SB, squared bias; NU, non-unity slope; LC, lack of correlation.

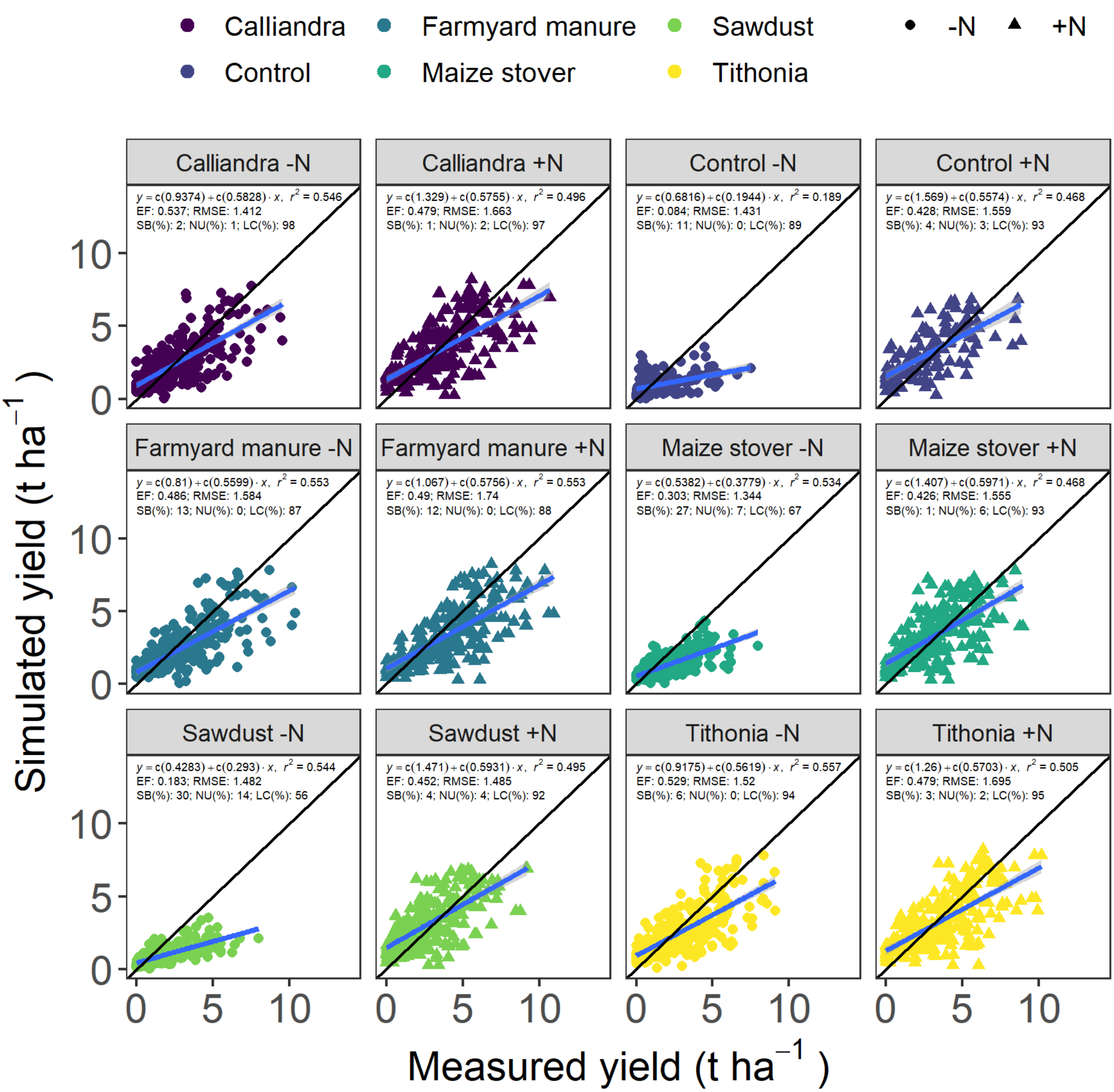


**Figure S7.** Treatment-specific simulated compared to measured maize grain yields at the four study sites for the calibrated parameter set by leave-one-site-out cross-validation. Abbreviations: EF, Nash-Sutcliffe model efficiency; RMSE, root mean squared error; SB, squared bias; NU, non-unity slope; LC, lack of correlation.

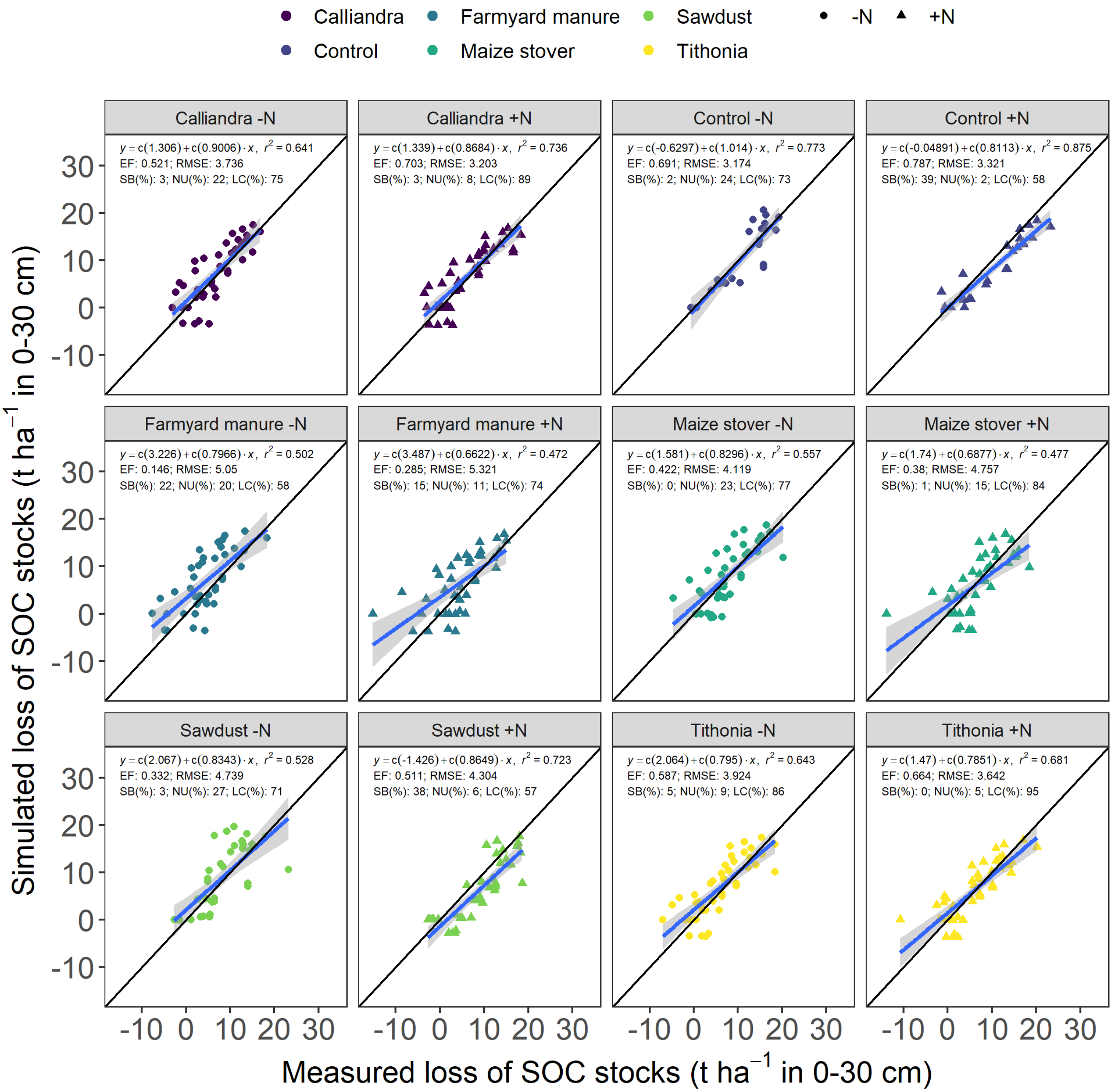


**Figure S8.** Treatment-specific simulated compared to measured changes in SOC stocks (without the Machanga site) since the start of the experiment at the four study sites for the calibrated parameter set by leave-one-site-out cross-validation. Abbreviations: EF, Nash-Sutcliffe model efficiency; RMSE, root mean squared error; SB, squared bias; NU, non-unity slope; LC, lack of correlation.

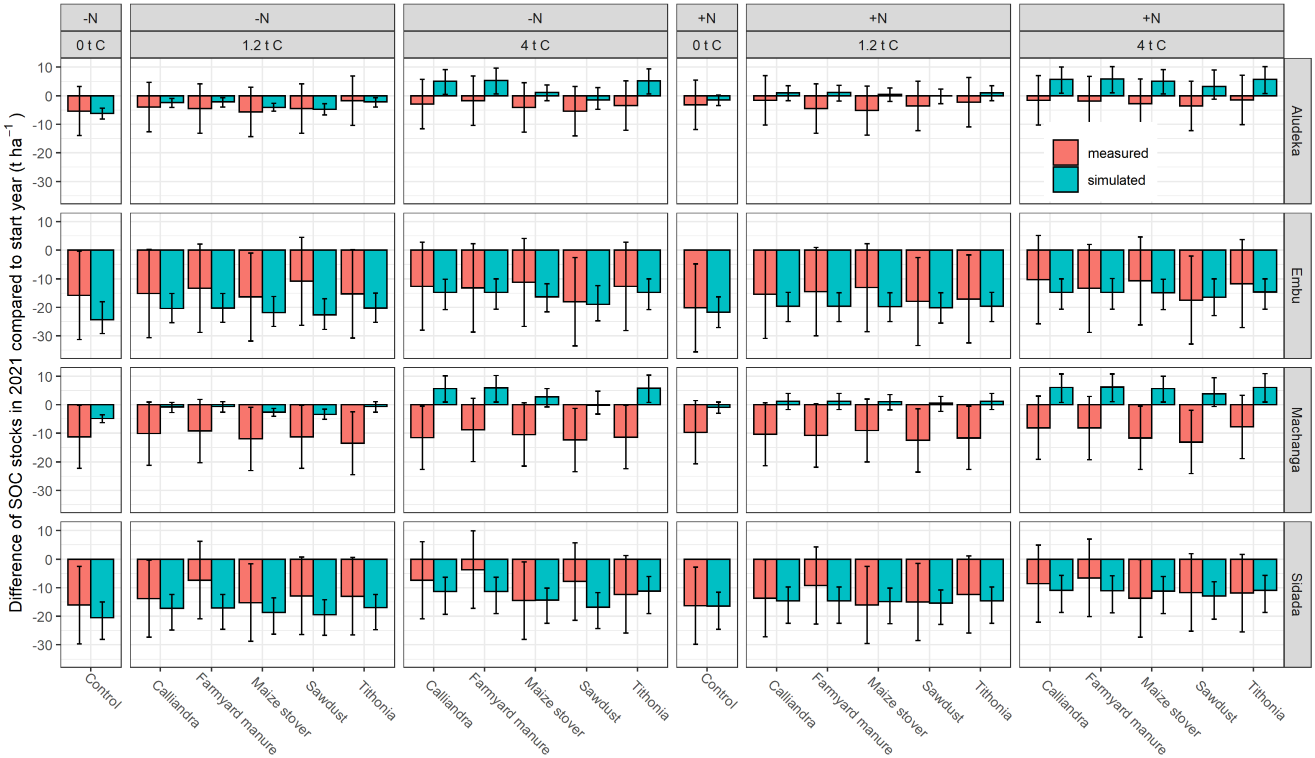


**Figure S9.** Barplots of simulated and measured change of SOC stocks (0-30 cm depth) until 2021 from cross-validation, at the four study sites for the different organic resource and chemical nitrogen fertilizer treatments. Error bars represent 95% confidence intervals based on BC (simulations) and variance (measurements).

## S5 $N_2O$ emissions

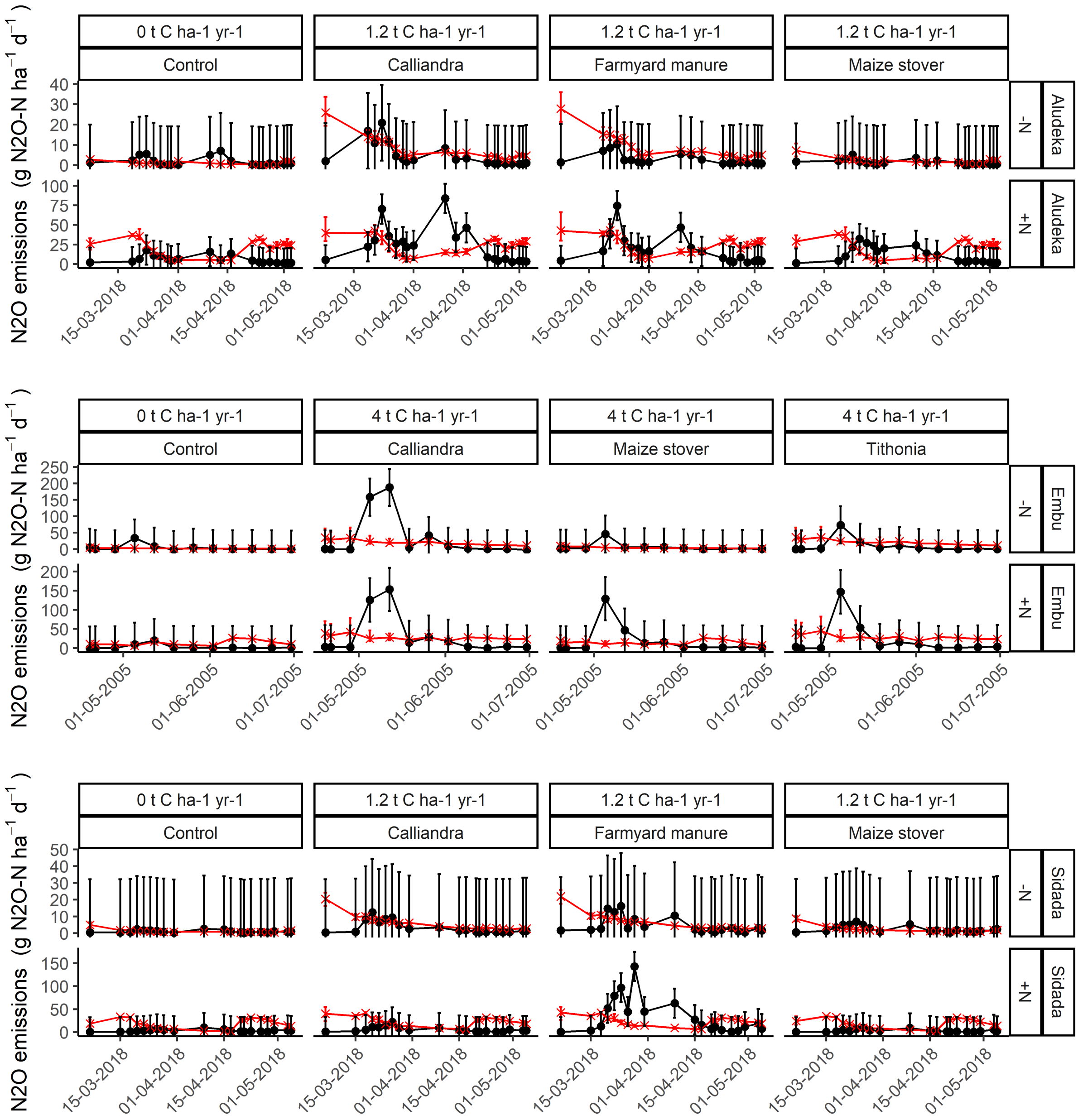


**Figure S1.** Example of the temporal development of measured (black) vs simulated (red) $N_2O$ emissions by site. The black error bars represent the 95% confidence intervals due to spatial replication error, the red error bars represent the 95% credibility intervals of simulated $N_2O$ emissions resulting from parameter distribution of the posterior parameter set.

## References


FAO: World reference base for soil resources, no. 84 in World Soil Resources Report, FAO, Rome, 1998.

Hodnett, M. G. and Tomasella, J.: Marked differences between van Genuchten soil water-retention parameters for temperate and tropical soils: a new water-retention pedo-transfer functions developed for tropical soils, Geoderma, 108, 155–180, https://doi.org/10.1016/S0016-7061(02)00105-2, 2002.

Laub, M., Schlichenmeier, S., Vityakon, P., and Cadisch, G.: Litter Quality and Microbes Explain Aggregation Differences in a Tropical Sandy Soil, Journal of Soil Science and Plant Nutrition, 22, 848–860, https://doi.org/10.1007/s42729-021-00696-6, 2022.

Laub, M., Corbeels, M., Couëdel, A., Ndungu, S. M., Mucheru-Muna, M. W., Mugendi, D., Necpalova, M., Waswa, W., Van de Broek, M., Vanlauwe, B., and Six, J.: Managing soil organic carbon in tropical agroecosystems: evidence from four long-term experiments in Kenya, SOIL, 9, 301–323, https://doi.org/10.5194/soil-9-301-2023, publisher: Copernicus GmbH, 2023.

Palm, C., Gachengo, C. N., Delve, R. J., Cadisch, G., and Giller, K. E.: Organic inputs for soil fertility management in tropical agroecosystems: application of an organic resource database, Agriculture, Ecosystems & Environment, 83, 27–42, https://doi.org/10.1016/S0167-8809(00)00267-X, 2001.

Saxton, K. E. and Rawls, W. J.: Soil Water Characteristic Estimates by Texture and Organic Matter for Hydrologic Solutions, Soil Science Society of America Journal, 70, 1569–1578, https://doi.org/https://doi.org/10.2136/sssaj2005.0117, 2006.

van Genuchten, M.: A comparison of numerical solutions of the one-dimensional unsaturated—saturated flow and mass transport equations, Advances in Water Resources, 5, 47–55, https://doi.org/10.1016/0309-1708(82)90028-8, 1982.